



Transient heat transfer due to exponentially increasing heat inputs for turbulent flow of FC-72 in small diameter tubes

Li, Yantao
Fukuda, Katsuya
Liu, Qiusheng

(Citation)

International Journal of Heat and Mass Transfer, 110:880-889

(Issue Date)

2017-07

(Resource Type)

journal article

(Version)

Accepted Manuscript

(Rights)

© 2017 Elsevier.

This manuscript version is made available under the CC-BY-NC-ND 4.0 license
<http://creativecommons.org/licenses/by-nc-nd/4.0/>

(URL)

<https://hdl.handle.net/20.500.14094/90004448>



Transient heat transfer due to exponentially increasing heat inputs for turbulent flow of FC-72 in small diameter tubes

Yantao Li, Katsuya Fukuda, Qiusheng Liu

Graduate School of Maritime Sciences, Kobe University, 5-1-1, Fukaeminami, Higashinada, Kobe 658-0022, Japan

Abstract: The transient heat transfer process due to exponentially increasing heat inputs for turbulent flow of FC-72 was schematically investigated for different combinations of parameters such as flow velocity, inlet liquid temperature and period of exponentially increasing heat inputs. The ranges of Reynolds number, Re_d , and Prandtl number, Pr , were 23,400 to 81,800 and 8.4 to 10.8, respectively. The test heaters used in this study were circular SUS304 tubes with small inner diameters of 1, 1.8 and 2.8 mm, wall thickness of 0.5 mm, and heated lengths around 30, 40 and 50 mm. The effects of flow velocity, exponential period and tube inner diameter on transient turbulent heat transfer process were discussed in detail. It was clarified that the transient turbulent heat transfer due to exponentially increasing heat inputs could be analyzed by introducing a dimensionless time, Fourier number, Fo . An empirical correlation for transient turbulent heat transfer caused by exponentially increasing heat inputs on small diameter tubes was developed based on the effects of Fo , flow velocity and tube inner diameter. The empirical correlation presents the experimental data within $\pm 25\%$.

Keywords: FC-72, Transient heat transfer, Small diameter tubes, Turbulent flow, Exponentially increasing heat inputs.

1. Introduction

An in-depth knowledge of transient forced convection heat transfer has become important for the precise thermal management of high-performance electrical machines, nuclear reactors and renewable energy applications like thermal solar panels [1-4]. The dynamic processes such as start-up, shut-down, power surge, and pump failure may cause thermal transients, leading to high temperature gradients and severe thermal stress. The unsteady nature of thermal load imposes a challenge in maintaining the efficiency and reliability of the applications mentioned above. Therefore, a better understanding of the transient forced convection heat transfer process for time dependent heat generation is deemed necessary for safety assessment and optimal design of the thermal components involved in the dynamic process.

A great many experimental, analytical and numerical studies have focused on the transient laminar forced convection heat transfer. Sparrow and Siegel [5] conducted an analysis of transient laminar convection in the thermal entrance region of circular tubes. They determined thermal responses to unit step changes in the wall heat flux or in the temperature. Siegel [6] analyzed transient laminar forced convection in a parallel plate channel. The results demonstrated that the slug assumption did reveal the essential physical behavior of the systems considered,

although the numerical results were somewhat in error. Fakoor-Pakdaman et al. [7, 8] analytically and experimentally studied the transient laminar forced convection heat transfer inside a circular tube under time-dependent heat flux. They expressed the transient Nusselt number as a function of dimensionless space and time. The dimensionless time was defined as $Fo = \alpha t / r_i^2$, where Fo , α , t , r_i are the Fourier number, thermal diffusivity, elapsed time and tube inner radius, respectively. Semi-analytical relationships were developed on the basis of experimental data and analytical methodology to predict the transient thermal response.

Although there are some analytical and experimental studies on transient turbulent heat transfer, only a few are focused on the transient process caused by an exponentially increasing heat generation rate, $Q (=Q_0 \exp(t/\tau))$, where, Q_0 is initial heat generation rate, t is time, and τ is the exponential period of heat generation rate). Kakaç [9] numerically analyzed transient heat transfer for turbulent flow between two parallel plates for dynamic wall flux or wall temperature. The variation of the Nusselt number was presented in terms of non-dimensional space and time. The dimensionless time was defined as $Fo = \alpha t / (D_h/2)^2$, where D_h was the hydraulic diameter of the parallel-plate channel. Soliman and Johnson [10] analytically and experimentally studied the transient mean wall temperature change of a flat plate heated by an

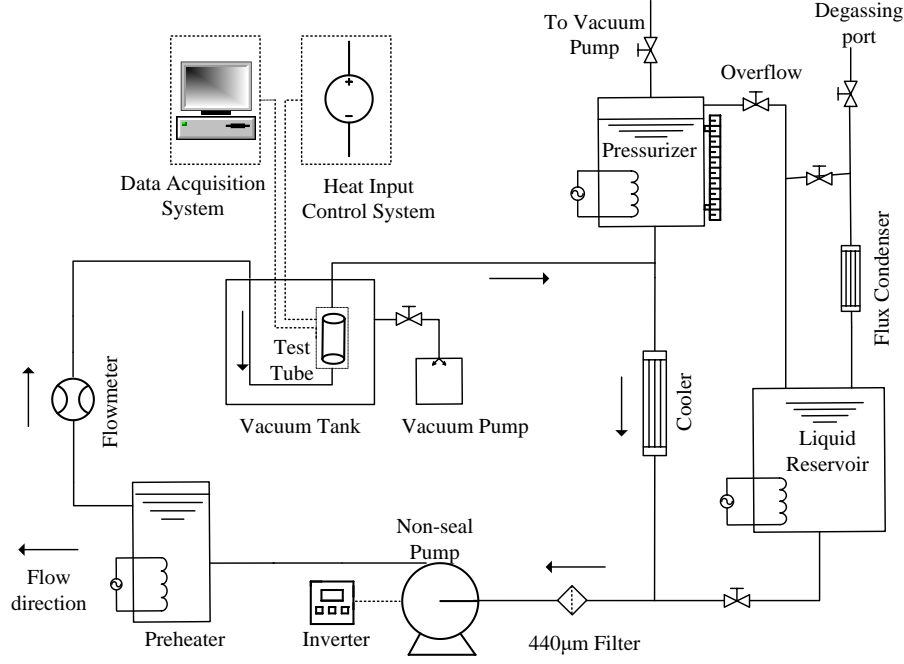


Fig. 1 Schematic diagram of experimental apparatus

exponential heat source. Their solutions were 50% higher than the experimental data. Kataoka et al. [11] investigated the transient phenomenon due to exponentially increasing heat inputs with water flowing over a platinum wire inserted in a round tube. They derived the transient Nusselt number correlation by introducing one non-dimensional parameter, $\tau u/L$ (where τ , u and L represent period, velocity and heater length, respectively). Liu et al. [12-15] conducted transient experiments for parallel flow of helium gas over horizontal cylinders, flat plates and twisted plates at various exponential periods of heat generation rates. Transient heat transfer correlations were obtained for various of heater configurations. Hata et al. [16] experimentally studied the transient turbulent heat transfer coefficients for water flow in tubes with relatively large inner diameters. An empirical correlation for describing the transient turbulent heat transfer was developed in terms of a non-dimensional exponential period. Although the correlation could represent the experimental data well, the non-dimensional exponential parameter seems to be meaningless for single-phase heat transfer.

The literature reviews above indicate that:

1) Many experimental studies of transient forced convection heat transfer were conducted with water or gas. There has been a lack of systematic experimental data on FC-72 flowing in tubes. FC-72 is expected to be an ideal coolant for electronical devices due to its high thermal

conductivity, low viscosity and super dielectric characteristics.

2) There are few experimental studies on transient turbulent heat transfer due to exponentially increasing heat generation rate with liquid flowing in small diameter (min-scale) tubes. The effects of the period of heat generation rate, velocity and tube size on the transient heat transfer still need to be clarified.

In this research, a systematical experiment has been performed on the transient turbulent heat transfer process for different combinations of parameters such as flow velocity, inlet liquid temperature and period of exponentially increasing heat input on small tubes with different inner diameters and heated lengths. The objectives are to obtain transient data under various experimental conditions, discuss the physical mechanism of transient turbulent heat transfer, and then develop empirical correlations for transient turbulent heat transfer caused by exponentially increasing heat inputs on small diameter tubes.

2. Experimental apparatus and methods

2.1 Experimental apparatus

The experimental apparatus used in this investigation is schematically illustrated in Fig. 1. Further details are described in previous work [17]. It is mainly composed of three primary subsystems: a flow loop section, a heat input control system and a data reduction system. The flow loop

was connected with 6.35-mm-diameter stainless steel tubes and Swagelok fittings, which could withstand system pressure up to 1 MPa. A canned type non-seal pump was used to circulate liquid through a previously vacuumed loop, marked with arrows in Fig. 1. A precision vortex flow meter located upstream of the test section was used to measure the flow rate. An inverter was set to regulate the frequency of a three-phase alternating power source to the circulation pump, thereby providing a means for fine adjustment of flow velocity. The desired inlet liquid temperature was controlled by a preheater or a cooler (a low temperature cryostat). The system pressure was established by saturated vapor partially filled in the pressurizer. The pressure could be adjusted and maintained within 1 kPa of a desired value by heating the liquid in the pressurizer to the corresponding saturation temperature. The test section was positioned in a vacuum tank to minimize convective heat loss from the test tube to the surroundings.

2.2 Test section

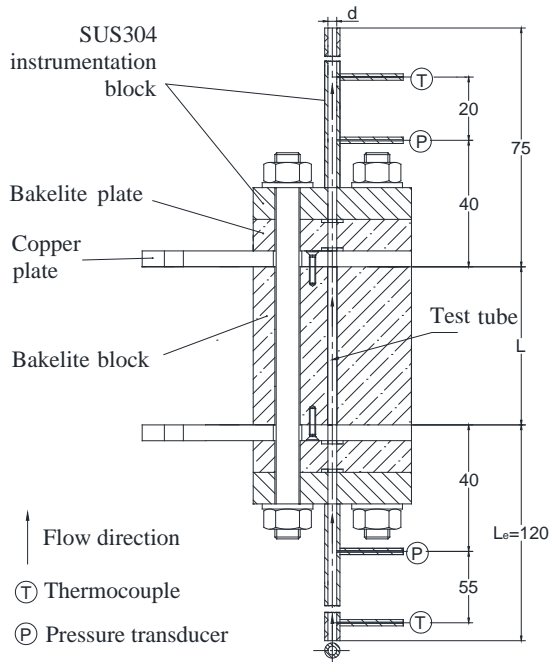


Fig. 2 Test section

The structure and dimensions of the test section assembly are shown in Fig. 2. The test heaters used in this study were circular SUS304 tubes with inner diameters, d , of 1, 1.8 and 2.8 mm, wall thickness, δ , of 0.5 mm, heated lengths, L , around 30, 40 and 50 mm, and a commercial finish inner surface condition as tabulated in Table 1. The test tube was soldered to copper plates at each end. Solder joints with very low resistance provided a good seal between the test tube

and the copper plates under high pressure and high temperature. The copper plates served as electrodes to provide a resistance free path for introducing direct current from the power source to the test tube. Protective Bakelite blocks were used to avoid mechanical vibrations or distortion of the small diameter test tube. The Bakelite plates insulated the test tube from the loop both electrically and thermally. Gaskets were used as a high pressure seal between the copper plates, insulating Bakelite plates and SUS304 instrumentation blocks. All the plates and blocks were clamped together with four steel bolts. In order to secure electrical and thermal isolation between the bolts and copper plates, PTFE sleeves were used to separate them from each other. The SUS304 instrumentation blocks provided a convenient connection of thermocouples and pressure transducers using standard compression fittings. Two 1-mm-diameter K-type thermocouples were arranged at the inlet and outlet of the test tube to measure the inlet and outlet liquid temperatures. The exact voltage-temperature relation of each thermocouple was calibrated by placing the probe in a controlled, uniform-temperature water tank. The inlet and outlet pressures were measured by two strain gauge transducers, located at a position 40 mm upstream and 40 mm downstream from the tube inlet and outlet points. The detailed locations for temperature and pressure measurement are shown in Fig. 2.

The test section was vertically oriented along the centerline of the flow channel with liquid flowing upward. Before entering the test tube, the liquid flows through an entrance region which has the same diameter as the inner diameter of the test tube to create a fully developed turbulent flow. In this study, the entrance region length, L_e , was given as 120 mm ($L_e/d=120$, 66.7 and 42.8 for $d=1$, 1.8 and 2.8 mm, respectively), which was assumed to be sufficient to secure fully developed hydrodynamic conditions according to the well-accepted correlation [18] as follows:

$$L_e/d = 4.4 \text{Re}^{1/6} \quad (1)$$

Table 1 Dimensions of test heaters

d (mm)	L (mm)	L/d ratio	δ (mm)
1	31.1, 40, 50	31.1, 40, 50	0.5
1.8	30.1, 40.2, 49.9	16.7, 22.3, 27.7	0.5
2.8	31.3, 40.5, 50.2	11.2, 14.5, 17.9	0.5

2.3 Experimental methods and procedure

Figure 3 illustrates a block diagram of the power supply and data acquisition system which is essentially the same as in experiments performed by Sakurai [19] and Fukuda [20].

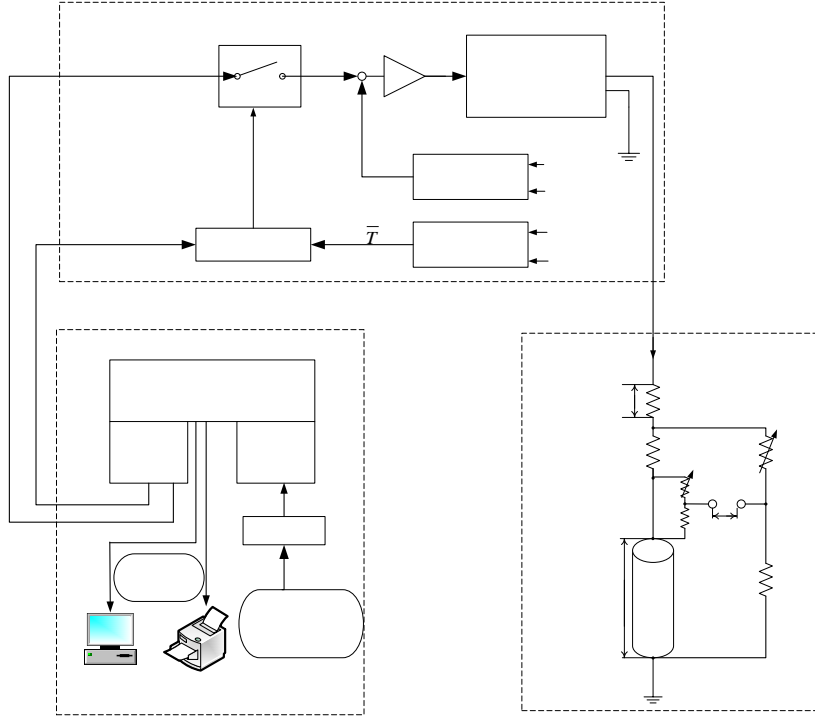


Fig. 3 Power supply and data acquisition system

Power cables from a fast response DC power supply (up to 1100 A and 15 V) were connected with copper electrodes to pass direct current to heat the test tube uniformly. The electrical resistance of the test tube was much smaller than the remainder of the electrical paths. Therefore, the overwhelming majority of the current was used to heat the test tube. The heat generation rate of the test tube was increased with a function of $Q=Q_0 \exp(t/\tau)$. A high speed analog computer calculated the instantaneous heat generation rate in the test tube and compared it with the heat input signal to ensure the two values were always equal.

The instantaneous heat generation rate for the test tube was calculated from the measured voltage differences between the two ends of the test tube and the current measured using Manganin standard resistance as shown by the next expression.

$$Q(t) = V_R(t) \frac{V_I(t)}{R_S} \quad (2)$$

The instantaneous average temperature of the test heater, $T_a(t)$, was measured by means of resistance thermometry using the test tube itself as a branch of a double bridge circuit. The unbalanced voltage of the double bridge circuit, $V_T(t)$, was generated by change of the tube resistance due to its temperature variation. $V_T(t)$ is expressed by the following equation.

$$V_T(t) = \frac{I(t)[R_2 R_T(t) - R_1 R_3]}{R_2 + R_3} \quad (3)$$

The unbalanced voltages of the double bridge circuit, $V_T(t)$, together with the voltage drops across the electrodes of the test section, $V_R(t)$, and that across a standard resistance, $V_I(t)$, were amplified and sent to a digital computer through a 16 bit analog to digital (A/D) converter. All these voltage signals were simultaneously sampled at a desired time interval by the A/D converter. The fastest sampling speed was 1 μ s/channel. The average temperature was obtained by means of the previously calibrated resistance-temperature relation in the following form.

$$R_T(t) = a(1 + bT_a(t) + cT_a(t)^2) \quad (4)$$

The instantaneous surface heat flux, $q(t)$, was then obtained from the following heat balance equation for a given heat generation rate. $q(t)$ means the difference between the heat generation rate per unit surface area and the change rate of energy storage in the test tube obtained from the faired average temperature versus time curve.

$$q(t) = \frac{V}{S} \left[Q(t) - \rho c \frac{dT_a(t)}{dt} \right] \quad (5)$$

where, ρ , c , V and S are the density, specific heat, volume and inner surface area of the test tube, respectively.

With the measured instantaneous average temperature and instantaneous surface heat flux of the test tube as conditions, the instantaneous tube inner surface temperature, $T_s(t)$, was calculated by solving the following unsteady heat conduction equation assuming the inner surface temperature to be distributed evenly.

$$\rho c \frac{\partial T}{\partial t} = \frac{1}{r} \frac{\partial}{\partial r} (r \lambda \frac{\partial T}{\partial r}) + \frac{1}{r} \frac{\partial}{\partial \theta} (\frac{\lambda}{r} \frac{\partial T}{\partial \theta}) + Q(t) \quad (6)$$

Calculation of Eq. (6) was carried out with PHOENICS code (version.2013) [21] using a digital computer. The boundary conditions are as follows:

$$q(t) = -\lambda \frac{\partial T}{\partial r} \Big|_{r=r_i} \quad (7)$$

$$\frac{\partial T}{\partial r} \Big|_{r=r_o} = 0 \quad (8)$$

The inlet and outlet pressures for the test tube were calculated from the pressures measured with inlet and outlet pressure transducers as follows:

$$P_{in} = P_{ipt} - (P_{ipt} - P_{opt}) \times \frac{0.04}{L + 0.08} \quad (9)$$

$$P_{out} = P_{in} - (P_{in} - P_{opt}) \times \frac{L}{L + 0.04} \quad (10)$$

All thermal physical properties were evaluated at the average bulk liquid temperature, T_L , $[= (T_{in} + (T_{out})_{cal})/2]$. Since the outlet temperature is measured at 60 mm downstream of the tube outlet, the measured temperature is slightly lower than the actual one due to heat loss caused by heat conduction. For better accuracy, the outlet liquid temperature, $(T_{out})_{cal}$, was calculated by the energy balance as follows:

$$(T_{out})_{cal} = T_{in} + \frac{4Lq}{uc_{p,l}\rho_l d} \quad (11)$$

The accuracies of the measured parameters including inlet flow velocity (u), inlet and outlet temperatures (T), inlet and outlet pressure (P), and exponential period (τ) are $\pm 3\%$, $\pm 1.5\text{K}$, $\pm 1\%$ and $\pm 2\%$, respectively. The experimental uncertainties of the derived values were calculated using the ANSI/ASME PTC 19.1-1985 [22]. The maximum uncertainties of the heat generation rate (Q), the tube inner surface temperature (T_s), the heat flux (q) and the heat transfer coefficient (h) were estimated to be $\pm 2\%$, $\pm 1\text{ K}$, $\pm 2.4\%$ and $\pm 4.4\%$, respectively. All the experimental errors and uncertainties are shown in Table 2.

The experiments were performed as in the following procedure. The flow loop components were adjusted to yield the desired flow velocity, inlet liquid temperature and system pressure as shown in Table 3. After the flow became stable, the power source was turned on. The heat input was

then increased exponentially with a certain exponential period. For each run, the inlet and outlet temperatures, T_{in} and T_{out} , the inlet and outlet pressures, P_{in} and P_{out} , the flow velocity, u , and other voltage signals accompanying the passage of time were recorded by the data acquisition system. Once the measured instantaneous average temperature, $T_a(t)$, exceeded the preset value, the current to the test tube was automatically cut off and this experimental run ended.

Table 2 Summary of experimental errors and uncertainties

Primary measurements		Derived quantities	
u	$\pm 3\%$	Q	$\pm 2\%$
T	$\pm 1.5\text{ K}$	T_s	$\pm 1\text{ K}$
P	$\pm 1\text{ kPa}$	q	$\pm 2.4\%$
τ	$\pm 2\%$	h	$\pm 4.4\%$

3. Experimental results and discussion

3.1 Experimental conditions

FC-72 was chosen as the working liquid. The details of the relevant properties were described in another paper [17]. The experiments were conducted at the flow velocities, u , changing from 8 to 11 m/s with corresponding Reynold number, Re_d , in the range of 23,400 to 45,900 for $d = 1\text{ mm}$, u changing from 3 to 6 m/s with corresponding Re_d in the range of 16,200 to 44,800 for $d = 1.8\text{ mm}$ and u changing from 3 to 7 m/s with corresponding Re_d in the range of 25,200 to 81,800 for $d = 2.8\text{ mm}$. The range of Prandtl number, Pr , was 8.4 to 10.8. Heat inputs to the test heater were exponentially increased with various exponential periods, τ . The inlet liquid temperatures, T_{in} , were maintained at 303, 323 and 343 K. The system pressure, P , was kept around 400 kPa for all experiment runs. The ranges of all experimental parameters are listed in Table 3.

3.2 Steady state turbulent heat transfer

Prior to study of transient turbulent heat transfer, it is important to know the steady state heat transfer characteristics under the same conditions. Steady state experiments were therefore performed before the transient experiments. The experimental results of steady state heat transfer of turbulent flow of FC-72 in small diameter tubes (mini-scale) were reported in previous work [17]. It was found that the steady state Nusselt numbers, $Nu_d (= hd/\lambda)$, for FC-72 flowing through small diameter tubes are higher than those predicted by classical correlations for conventional sized channels. The enhancement caused by the small sized

Table 3 Experimental conditions

$d(\text{mm})$	$u(\text{m/s})$	Re_d	Pr	$T_{in}(\text{K})$	$\tau(\text{s})$	$P(\text{kPa})$
1	8, 9, 10, 11	23,400 – 45,900	8.4 – 10.8	303, 323, 343	0.00273 – 15.5	400
1.8	3, 4, 5, 6	16,200 – 44,800	8.4 – 10.8	303, 323, 343	0.00157 – 14	400
2.8	3, 5, 7	25,200 – 81,800	8.4 – 10.8	303, 323, 343	0.00256 – 14.2	400

channels was explained by the conductive sublayer next to the tube inner surface. A steady state turbulent heat transfer correlation was developed by taking into account the effects of L/d , μ/μ_w , Pr and Re_d . The experimental data were correlated with an empirical correlation within $\pm 15\%$ deviation.

3.3 Transient turbulent heat transfer

3.3.1 Characteristics of heat generation rate, heat flux and surface temperature difference

Figure 4 shows typical time dependence of heat generation rate, Q , heat flux, q and surface temperature difference, $\Delta T_L (=T_s - T_L)$ at the inlet liquid temperature of 323 K, flow velocity of 11 m/s and exponential periods of 80.8 ms, 382.4 ms and 1.5 s, respectively. As shown in Fig. 4, heat flux and surface temperature difference increase exponentially with the increase of heat generation rate. A shorter period means a higher heat generation rate. Thus heat flux and surface temperature difference also increase more rapidly while the period is shorter. Those values increase slower when the period is longer.

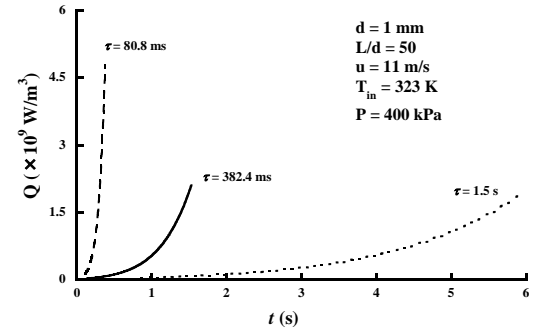
3.3.2 Transient heat transfer coefficient

The heat transfer coefficient, h , was expressed by the following equation:

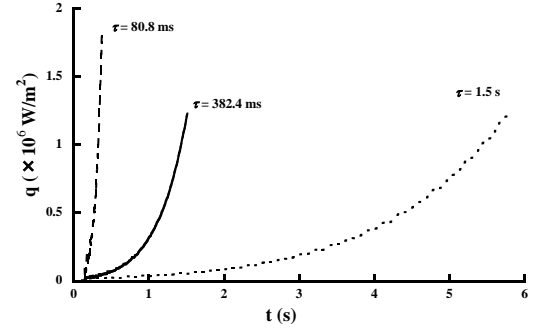
$$h = q / \Delta T_L \quad (12)$$

The instantaneous heat transfer coefficients were measured using a tube with inner diameter of 1.8 mm and heated length of 49.9 mm for flow velocity of 6 m/s, inlet liquid temperature of 323 K and exponential periods of 0.15, 1.4 and 13.9 s. The data was plotted against elapsed time and surface temperature difference in Fig. 5 and Fig. 6, respectively. As shown in those figures, the heat transfer coefficients dip and approach an asymptotic value at every period. Some researchers [23, 24] considered that the temperature is uniform in the liquid at the initial stage, the

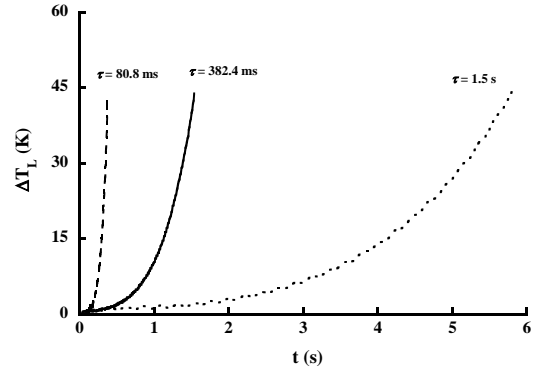
heat transfer coefficients were mainly determined by the transient conduction in the fluid. With the increase of thermal boundary layer and development of temperature



(a) Heat generation rate, Q



(b) Heat flux, q



(c) Surface temperature difference, ΔT_L

Fig. 4 Time dependency of Q , q and ΔT_L at various τ

distribution, the heat transfer coefficients approach the asymptotic value or steady state value. This process was influenced by the exponential periods of heat generation rate. It was also found that the transient heat transfer coefficients decrease and approach asymptotic values for all other experimental conditions. Particular attention should be paid to the asymptotic value for each exponential period. Thus the data at surface temperature differences of 20, 30, 40 and 50 K should be taken as representative data hereinafter.

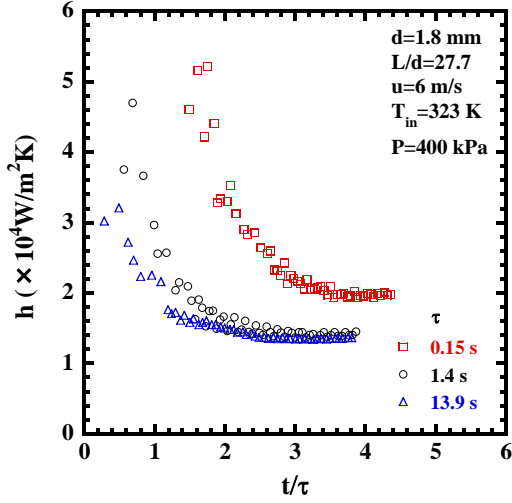


Fig. 5 Instantaneous h versus t/τ at different τ

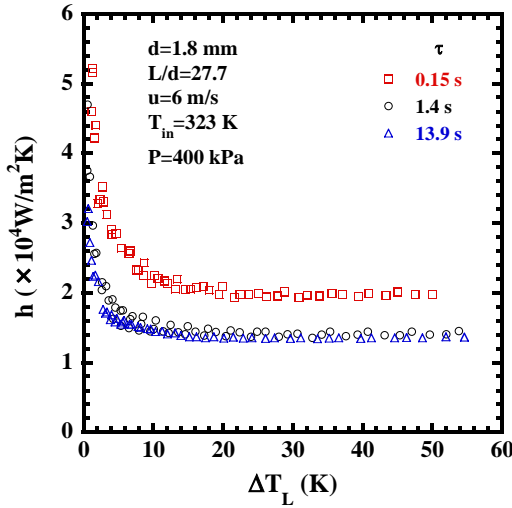


Fig. 6 Instantaneous h versus ΔT_L at different τ

Figure 7 shows the relation of heat transfer coefficients, h and the exponential periods, τ , with flow velocity, u , as a parameter. The heat transfer coefficients measured using 1 mm diameter tube for flow velocities of 8, 9, 10 and 11 m/s, and inlet temperature of 303 K were plotted with the surface temperature differences of 20, 30, 40 and 50 K. With the increase of exponential periods, the heat transfer coefficients gradually decrease and approach an asymptotic value at each velocity. This trend is similar to observations by other

researchers [14-16]. As shown In Fig. 7, both flow velocity and exponential period affect the transient heat transfer process.

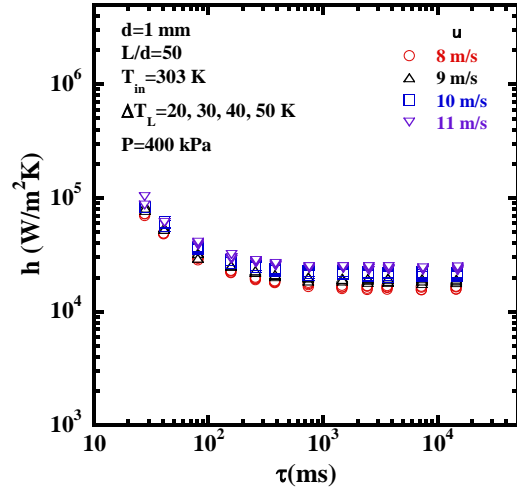


Fig. 7 h versus τ at various flow velocities for $d = 1$ mm

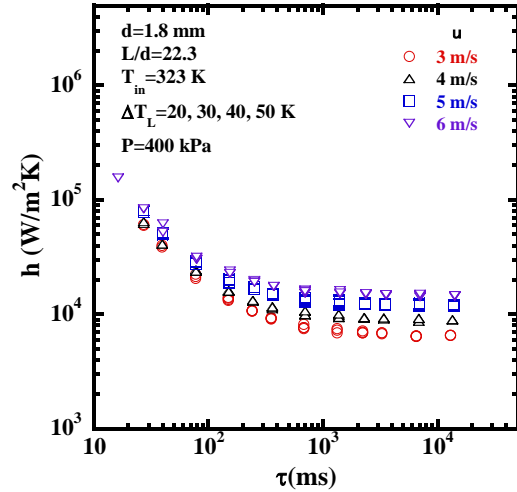


Fig. 8 h versus τ at various flow velocities for $d = 1.8$ mm

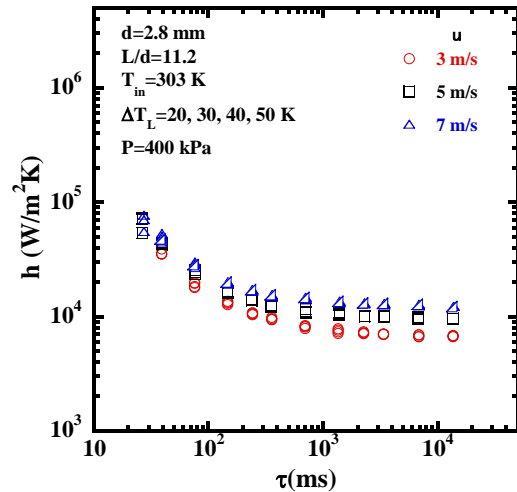


Fig. 9 h versus τ at various flow velocities for $d = 2.8$ mm

For periods larger than about 5 s, the increase of heat generation rate was so slow that the thermal boundary layer next to the tube inner surface was fully developed. The heat transfer coefficients did not depend upon the exponential period. Therefore, the experiments with exponential periods larger than 5 s can be practically regarded as steady state experiments. The experimental results for steady state heat transfer have been reported in previous work [17].

With a decrease of period from about 5 s, the heat transfer coefficients slightly increase. The region from period of 5 s to a period at which heat transfer coefficient is 5% larger than the steady state value is considered as quasi steady state. The quasi steady state region is from period of 5 s to period of about 1 s in Fig.7. In this region, the heat transfer coefficients become obviously higher for higher flow velocities. Meanwhile, the heat transfer coefficients approach the steady state for each velocity and they are weakly affected by the periods. It seems that the usual forced convection heat transfer predominates the heat transfer process. The heat transfer process in this region transports heat through the thermal boundary layer influenced by the liquid flow condition.

With further decrease of periods, the heat transfer coefficients gradually increase and they are much higher than that for steady state. This shows that the heat transfer process is in a transient state. The effect of heat conduction contribution increases gradually with a decrease of periods. And the heat transfer process is governed by conductive heat transfer rather than the convective heat transfer component for very short periods. This can be proven by the fact that the flow velocity has relatively small impact on heat transfer coefficients in the transient state region. Liu [15] stated that the development of thermal boundary layer is slower than the increment of wall temperature due to very high heat generation rate. The heat conduction is high due to thin thermal boundary layer and severe temperature gradients. The heat conduction contribution on heat transfer process for transient state is much higher than that for quasi steady state.

The same results were also found for the tubes with inner diameters of 1.8 and 2.8 mm as shown in Fig. 8 and Fig. 9.

3.3.3 Transient Nusselt number

The relations between heat transfer coefficients, h , and exponential periods, τ , shown in Fig.7 to Fig.9 were rewritten in the form of variations of Nusselt number, Nu_d , against Fourier number, Fo , in Fig.10 to Fig. 12 for comparison. The non-dimensional time, Fo , is defined as:

$$Fo = \frac{\alpha \tau}{r_i^2} \quad (13)$$

where α , τ , and r_i are the thermal diffusivity of liquid, exponential period, and the inner radius of test tube,

respectively.

As shown in Fig. 10 to Fig. 12, Nu_d also decrease and

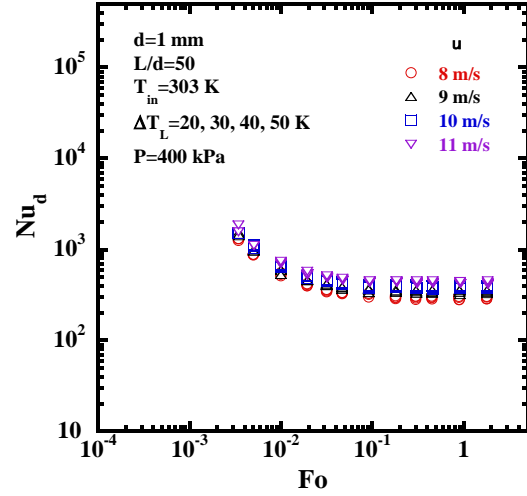


Fig. 10 Nu_d versus Fo at various flow velocities for $d = 1$ mm

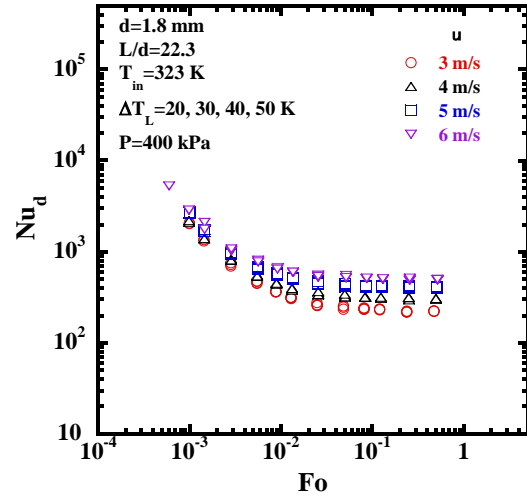


Fig. 11 Nu_d versus Fo at various flow velocities for $d = 1.8$ mm

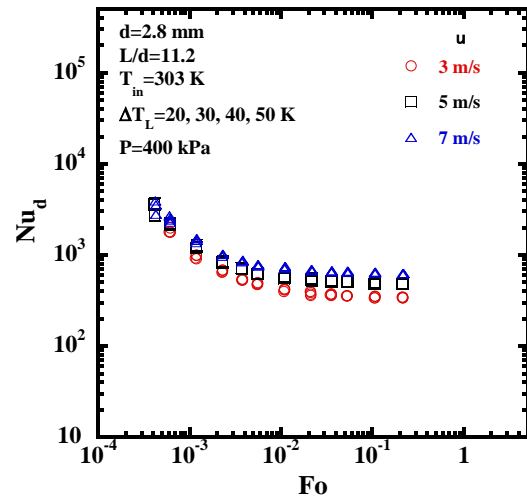


Fig. 12 Nu_d versus Fo at various flow velocities for $d = 2.8$ mm

approach an asymptotic value for each flow velocity. The flow velocity has clear influence on Nu_d for longer Fo , but exerts a relatively small effect on Nu_d for shorter Fo . The relation between Nu_d and Fo with flow velocity as a parameter shows the same trend as h versus τ for each velocity. Taking the aforementioned heat conduction contribution in the transient turbulent heat transfer process into consideration, it is reasonable to assume that the transient turbulent heat transfer characteristics could be described by introducing the non-dimensional time, Fo . As stated earlier, Fakoor-Pakdman [7, 8] employed Fo to analyse the transient laminar forced convection heat transfer inside a circular tube under time-dependent heat flux. Kakaç [9] also numerically analyzed transient heat transfer for turbulent flow using Fo . Therefore, the empirical correlation for transient turbulent heat transfer caused by exponentially increasing heat inputs will be derived later by taking the effect of the non-dimensional time, Fo into account.

3.3.4 Effect of Fo , u and d on transient turbulent heat transfer

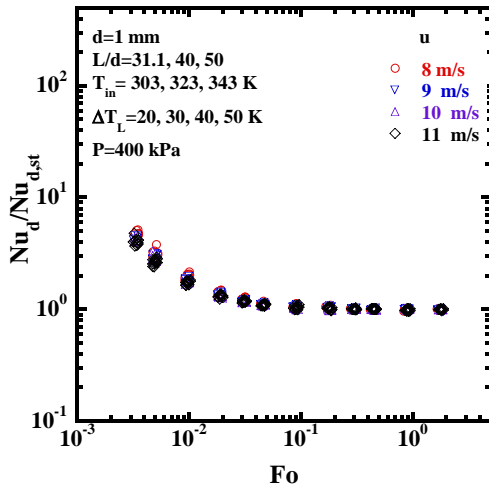


Fig. 13 $Nu_d/Nu_{d,st}$ versus Fo for $d=1$ mm

Figures 13 to 15 show the ratios of transient turbulent Nusselt numbers, Nu_d , to steady state ones, $Nu_{d,st}$, against Fo for all the data measured using tubes with inner diameters of 1, 1.8 and 2.8 mm, respectively. The $Nu_d/Nu_{d,st}$ ratios approach unity for larger Fo , which implies the heat transfer shifts to steady state heat transfer. And the $Nu_d/Nu_{d,st}$ ratios increase with the decrease in Fo for smaller Fo . This means the heat transfer shifts to transient heat transfer. The largest transient turbulent heat transfer data become almost 6, 11 and 10 times the steady state for tube inner diameters of 1, 1.8 and 2.8 mm, respectively. Therefore, the study of transient turbulent heat transfer is fundamentally important for improving the reliability and efficiency of dynamic heat

exchangers.

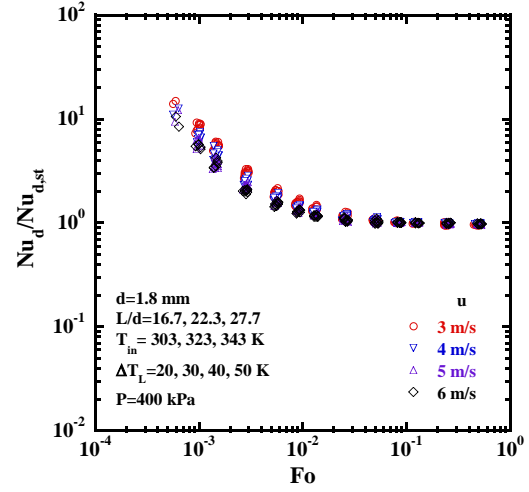


Fig. 14 $Nu_d/Nu_{d,st}$ versus Fo for $d=1.8$ mm

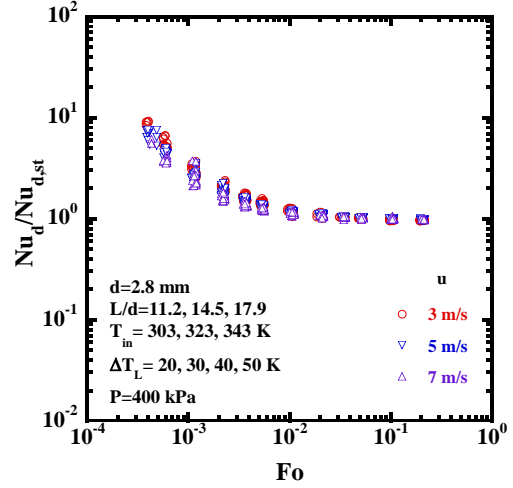


Fig. 15 $Nu_d/Nu_{d,st}$ versus Fo for $d=2.8$ mm

As mentioned earlier, the flow velocity, u , has a weak effect on transient heat transfer coefficient. The weak effect of flow velocity can also be observed in Fig. 13 to Fig. 15. It was found that the increment of transient Nusselt numbers relative to the steady state is higher for lower flow velocity. The effect of heat conduction contribution for transient state is higher for lower flow velocity. The heat conduction component is the maximum when the velocity is zero. Therefore, the increment of transient data relative to the steady state is higher for lower flow velocity.

The experimental data measured for tube inner diameters of 1, 1.8 and 2.8 mm under various experimental conditions were plotted in Fig. 16. The ratios of transient turbulent Nu_d to steady state one for three tube inner diameters all increase with a decrease of Fo . However, the effect of heat conduction contribution for transient state increases with a

decrease of tube inner diameter. Thus, the increment of transient state data relative to the steady state is higher for smaller diameter.

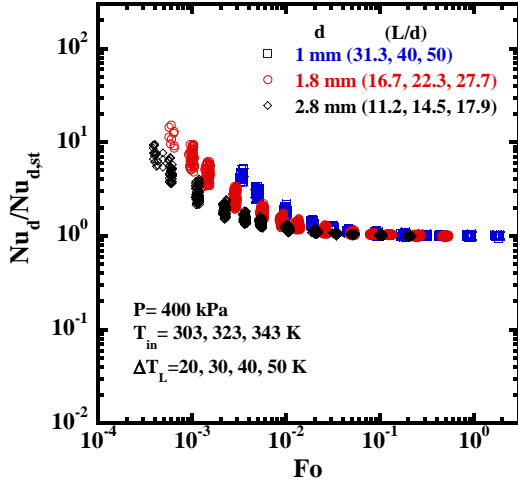


Fig. 16 $Nu_d/Nu_{d,st}$ versus Fo for $d = 1, 1.8$ and 2.8 mm

3.3.5 Transient turbulent heat transfer correlation

The transient turbulent heat transfer correlation for a wide range of exponentially increasing heat inputs on small diameter tubes has been developed by combining the steady state values with effects of the Fo , flow velocity and tube inner diameter clarified in this work. It is expressed as follows:

$$Nu_d = Nu_{d,st} (1 + C \cdot Fo^{-1.2}) \quad (14)$$

where, C is a constant to accommodate the effect of flow velocity and tube inner diameter. It is expressed in the following equation.

$$C = m \left(\frac{u}{u_0} \right)^n \left(\frac{d}{d_0} \right)^{-1.73} \quad (15)$$

where, d_0 ($=0.001$ m) and u_0 ($=3$ m/s) are the reference diameter and reference velocity. The constants of m and n are determined as follows: $m=3.9 \times 10^{-3}$ and $n=-0.51$ for 2.8 mm diameter tube; $m=4.9 \times 10^{-3}$ and $n=-0.88$ for 1.8 mm diameter tube and $m=6.5 \times 10^{-3}$ and $n=-0.56$ for 1 mm diameter tube.

Figure 17 shows the ratios of the experimental transient turbulent heat transfer data to the values calculated from transient turbulent heat transfer correlation, Eq. (14) and Eq. (15), versus Fo for tube inner diameters of $1, 1.8$ and 2.8 mm, inlet liquid temperatures of $303, 323$ and 343 K, surface temperature differences of $20, 30, 40$ and 50 K and various flow velocities. For larger Fo , the data show a smaller deviation from the correlation because they

approach the steady state. For steady state, the heat transfer process is governed by the usual heat convection and the heat conduction component is almost none. With a decrease of Fo , the heat transfer process becomes a complicated phenomenon combining both heat convection and heat conduction. The heat transfer process may be affected by other factors besides Fo , flow velocity and inner diameter. Thus the data for smaller Fo show a relatively larger deviation from the proposed empirical correlation considering only the effects of Fo , flow velocity and inner diameter. The obtained empirical correlation represents all those experimental data (3253 points) within $\pm 25\%$.

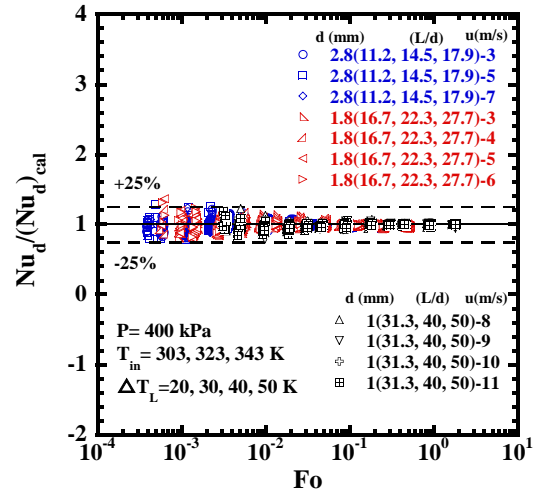


Fig. 17 $Nu_d/(Nu_d)_{cal}$ versus Fo for $d=1, 1.8$ and 2.8 mm

4. Conclusions

Transient turbulent heat transfer caused by various exponentially increasing heat inputs was experimentally investigated for several flow velocities and inlet liquid temperatures for small diameter tubes with different inner diameters and heated lengths at a certain pressure. The experimental results lead to the following conclusions:

- 1) The usual convective heat transfer dominates the heat transfer process for quasi steady state region. The heat conduction gradually governs the heat transfer process for transient state with a decrease of period.
- 2) It was clarified that the transient heat transfer process could be analyzed in terms of the dimensionless time, Fo .
- 3) The ratios of $Nu_d/Nu_{d,st}$ approach unity for larger Fo , and they increase with the decrease in Fo for smaller Fo .
- 4) The increment of transient state data relative to the steady state is higher for lower velocity as the effect of heat conduction contribution is higher for lower velocity.
- 5) The increment of transient state data relative to the steady state is higher for smaller diameter as the effect of

heat conduction contribution increases with a decrease of tube inner diameter.

6) Based on the effects of Fo , flow velocity and tube inner diameter, the empirical correlation of transient turbulent heat transfer was developed for a wide range of exponentially increasing heat inputs using small diameter tubes. Deviations between the experimental data and the empirical correlation were less than $\pm 25\%$.

Nomenclature

a, b, c	constant in Eq. (4)
C	constant in Eq. (14)
c_p	specific heat at constant pressure, J/kg K
d	inner diameter of the test tube, m
d_0	reference diameter, 0.001 m
D_h	hydraulic diameter of a parallel-plate channel
Fo	$=\alpha t/r_i^2$, Non-dimensional time, Fourier number
h	heat transfer coefficient, W/m ² K
I	current flowing through standard resistance, A
L	heated length, m
L_e	entrance length, m
m, n	constant in Eq. (15)
Nu_d	$=hd/\lambda$, Nusselt number, transient Nusselt number
$Nu_{d,st}$	steady state Nusselt number
$(Nu_d)_{cal}$	calculated Nusselt number
P	pressure, kPa
P_{in}	pressure at inlet of heated section, kPa
P_{ipt}	pressure measured by inlet pressure transducer, kPa
P_{out}	pressure at outlet of heated section, kPa
P_{opt}	pressure measured by outlet pressure transducer, kPa
Pr	$=c_p\mu/\lambda$, Prandtl number
Q	heat input per unit volume, W/m ³
Q_0	initial exponential heat input, W/ m ³
q	heat flux, W/m ²
r	test tube radius, m
r_i	test tube inner radius, m
r_o	test tube outer radius, m
R_1 to R_3	resistance in a double bridge circuit, Ω
Re_d	$=ud/\nu$, Reynolds number
R_s	resistance of standard resistance, Ω
R_T	resistance of test tube, Ω
S	surface area, m ²
T	temperature, K
T_{in}	inlet liquid temperature, K
T_L	average bulk liquid temperature, K
T_{out}	outlet liquid temperature, K
$(T_{out})_{cal}$	calculated outlet liquid temperature, K
T_s	heater inner surface temperature, K

ΔT_L	$=(T_s-T_L)$, surface temperature difference between heater inner surface temperature and average bulk liquid temperature, K
t	time, s
u	flow velocity, m/s
u_0	reference flow velocity, m/s
V	volume, m ³
V_{FM}	voltage signal of flow velocity, V
V_I	voltage drop across standard resistance, V
V_R	voltage drop across the test heater, V
V_I	unbalance voltage of a double bridge circuit, V
V_{TLi}	voltage signal of inlet temperature
V_{TLo}	voltage signal of outlet temperature
α	thermal diffusivity, m ² /s
δ	wall thickness, m
λ	thermal conductivity, W/mK
μ	viscosity, Ns/m ²
μ_w	viscosity at tube wall temperature, Ns/m ²
ρ	density, kg/m ³
τ	exponential period, s

Subscripts

a	average
cal	calculated
h	hydraulic
in	inlet
out	outlet
L	liquid
s	surface
st	steady state

References

- [1] A. Boglietti, S. Member, A. Cavagnino, D. Staton, M. Shanel, M. Mueller, and C. Mejuto, Evolution and modern approaches for thermal analysis of electrical machines, IEEE Trans. Ind. Elect., 56(3), (2009) 871–882.
- [2] Xiuqing Li, Renaud Le Pierres, Stephen John Dewson, Heat exchangers for the next generation of nuclear reactors, Proceedings of ICAPP '06 Reno, NV USA, June 4–8, (2006).
- [3] J. B. Garrison, Optimization of an integrated energy storage scheme for a dispatchable solar and wind powered energy system," Proceedings of the ASME 6th International Conference on Energy Sustainability, San Diego, CA, July 23–26, (2012).
- [4] K. Bennion and M. Thornton, Integrated vehicle thermal management for advanced vehicle propulsion technologies : Integrated vehicle thermal management for advanced vehicle

- propulsion technologies, NREL report, (2010) 1–15.
- [5] E. M. Sparrow, and R. Siegel, Thermal entrance region of a circular tube under transient heating conditions,” Third U. S. National Congress of Applied Mechanics, (1958) 817–826.
- [6] R. Siegel, , Heat transfer for laminar flow in ducts with arbitrary time variations in wall temperature, Trans. ASME, 27(2), (1960) 241–249.
- [7] M. Fakoor-Pakdaman, M. Ahmadi, M. Bahrami, Unsteady laminar forced-convective tube flow under dynamic time-dependent heat flux, J. Heat Transfer, 136, (2014) 041706-1-9.
- [8] M. Fakoor-Pakdaman, M. Ahmadi, M. Bahrami, Temperature-aware time-varying convection over a duty cycle for a given system thermal-topology, Int. J. Heat Mass Transf. 87, (2015) 418–428.
- [9] S. Kakaç, Transient forced convection heat transfer in a channel, Wärme- und Stoffübertragung, Vol. 1, (1968) 169-176.
- [10] M. Soliman, H.A. Johnson, Transient heat transfer for forced convection flow over a flat plate of appreciable thermal capacity and containing an exponential time-dependent heat source. Int. J. Heat Mass Transf. 11(1), (1968) 27–38.
- [11] I. Kataoka, A. Serizawa, A. Sakurai, Transient boiling heat transfer under forced convection. Int. J. Heat Mass Transfer 26(4), (1983) 583–595.
- [12] Q. Liu, K. Fukuda, Transient heat transfer for forced convection flow of helium gas. JSME Int. J. Ser B 45(3), (2002) 559–564.
- [13] Q. Liu, K. Fukuda, Z. Zheng, Theoretical and experimental studies on transient heat transfer for forced convection flow of helium gas over a horizontal cylinder. JSME Int. J. Ser B, (2006).
- [14] Q. Liu, Z. Zhao, K. Fukuda, Transient heat transfer for forced flow of helium gas along a horizontal plate with different widths, Int. J. Heat Mass Transf. 75, (2014) 433–441.
- [15] Q. Liu, Z. Zhao, K. Fukuda, Experimental study on transient heat transfer enhancement from a twisted plate in convection flow of helium gas, Int. J. Heat Mass Transf. 90, (2015) 1160–1169.
- [16] K. Hata, N. Kai, Y. Shirai, S. Masuzaki, Transient turbulent heat transfer for heating of water in a short vertical tube, J. Power Energy Syst. 5, (2011) 414–428.
- [17] Y. Li, K. Fukuda, Q. Liu, M. Shibahara, Turbulent heat transfer with FC-72 in small diameter tubes, Int. J. Heat Mass Transf. 103, (2016) 428–434.
- [18] Frank M. White., Fluid Mechanics, 8th Edition. McGraw-Hill Education, (2015) 31
- [19] A. Sakurai, and M. Shiotsu, Transient pool boiling heat transfer, Part 1: incipient boiling superheat”, ASME J. Heat Transfer, (1977) 547-553.
- [20] K. Fukuda, Q. Liu, Steady and transient critical heat fluxes on a horizontal cylinder in a pool of Freon-113, Int. J. Trans Phenom. 7 (2006) 71–83.
- [21] D.B. Spalding., The PHOENICS Beginner’s Guide, CHAM Ltd., London, United Kingdom, (2013).
- [22] ANSI/ASME PTC 19.1-1985, Measurement Uncertainty, Supplement on Instruments and Apparatus, Part 1, (1987).
- [23] R.C.C.Wang, B.T.F. Chung and L.C. Thomas, Transient convective heat transfer for laminar boundary layer flow with effects of wall capacitance and resistance, J. Heat Transfer 99(4), (1977) 513-519.
- [24] H. Kawamura, Experimental and analytical study of transient heat transfer for turbulent flow in a circular tube, Int. J. Heat Transfer, vol. 20, (1977) 443-450.